Title
First Implantation of Silicon Nanopore Membrane Hemofilters

Journal
ASAIO Journal, 62(4)

ISSN
1058-2916

Authors
Kensinger, Clark
Karp, Seth
Kant, Rishi
et al.

Publication Date
2016-07-01

DOI
10.1097/mat.0000000000000367

Peer reviewed

Published in final edited form as:

ASAIO J. 2016 ; 62(4): 491–495. doi:10.1097/MAT.0000000000000367.

First Implantation of Silicon Nanopore Membrane Hemofilters

Clark Kensinger, MD[*], **Seth Karp, MD**[*], **Rishi Kant, PhD**[†], **Benjamin W. Chui, PhD**[‡], **Kenneth Goldman**[§], **Torin Yeager**[†], **Edward R. Gould, MD**[**], **Amanda Buck, PhD**[‖,¶], **David C. Laneve**[‖], **Joseph J. Groszek**[**], **Shuvo Roy**[†], and **William H. Fissell, MD**[**]

[*]Department of Surgery, Vanderbilt University, Nashville, TN

[†]Department of Bioengineering and Therapeutic Sciences, University of California, San Francisco

[‡]Ben Chui Consulting, Sunnyvale, CA

[§]H-Cubed, Inc. Olmsted Falls, OH

[¶]Departments of Radiology and Radiological Sciences and Biomedical Engineering, Vanderbilt University, Nashville, TN

[‖]Department of Surgery, Vanderbilt University, Nashville, TN

[**]Nephrology and Hypertension, Vanderbilt University, Nashville, Tennessee

Abstract

An implantablehemofilter for the treatment of kidney failure depends critically on the transport characteristics of the membrane and the biocompatibility of the membrane, cartridge, and blood conduits. A novel membrane with slit-shaped pores optimizes the trade-off between permeability and selectivity, enabling implanted therapy. Sustained (3–8) day function of an implanted parallel-plate hemofilter with minimal anticoagulation was achieved by considering biocompatibility at the subnanometer scale of chemical interactions and the millimeter scale of blood fluid dynamics. A total of 400 nm-thick polysilicon flat sheet membranes with 5–8 nm 2 micron slit-shaped pores were surface-modified with polyethylene glycol. Hemofilter cartridge geometries were refined based on computational fluid dynamics predictions of blood flow. In an uncontrolled pilot study, silicon filters were implanted in six class A dogs. Cartridges were connected to the cardiovascular system by anastamoses to the aorta and inferior vena cava and filtrate was drained to collection pouches positioned in the peritoneum. Pain medicine and acetylsalicylic acid were administered twice daily until the hemofilters were harvested on postoperative days 3 (n = 2), 4 (n = 2), 5 (n = 1), and 8 (n = 1). No hemofilters were thrombosed. Animals treated for 5 and 8 days had microscopic fractures in the silicon nanopore membranes and 20–50 ml of transudative (albumin sieving coefficient 0.5 – 0.7) fluid in the collection pouches at the time of explant. Shorter experimental durations (3–4 days) resulted in filtration volumes similar to predictions based on mean arterial pressures and membrane hydraulic permeability and (~ 0.2 – 0.3), similar to

Correspondence: William H. Fissell, MD, Department of Nephrology and Hypertension, Vanderbilt University Medical Center, 2213 Garland Avenue, S3223 MCN, Nashville, TN 37232. william.fissell@vanderbilt.edu.

Disclosure: Drs. Fissell and Roy have certain rights to intellectual property and are founders of a biotech startup company related to these technologies.

Foundation Disclosures: WHF and SR have certain rights to intellectual property and are founders of a biotech startup company related to these technologies.

preimplantation measurements. In conclusion, a detailed mechanistic and materials science attention to blood–material interactions allows implanted hemofilters to resist thrombosis. Additional testing is needed to determine optimal membrane characteristics and identify limiting factors in long-term implantation.

Keywords

Hemofiltration; Nanotechnology; MEMS; Biocompatibility

Permanently implanted hemofilters for the treatment of kidney failure could reduce the risks of accidental disconnect, vascular access infection, and episodic rapid ultrafiltration (UF) rates that are present in maintenance hemodialysis. Coupled with a bioreactor of living renal tubule cells, an implanted hemofilter can constitute a bioartificial kidney similar to the renal assist device but much smaller. [1] In addition, if the patient's cardiovascular system is to be the only pump to circulate blood, an implanted filter must have very low arteriovenous pressure drop and high hydraulic permeability, as well as prolonged resistance to fouling and clotting. Polymer hollow-fiber dialyzer membranes have a distribution of pore sizes arising from the thermodynamics of the manufacturing process.[2,3] The largest pores in the distribution dominate transport processes, so in practice, hemofiltration membranes are engineered such that even the largest pores are small enough to retain albumin. The majority of pores are much smaller than the molecular weight cutoff of the membrane, and thus much smaller than actually needed to retain proteins. This severely limits the hydraulic permeability of the membranes. A completely new technology approach to membrane fabrication allows the engineer to precisely control the size and shape of each pore individually. Silicon micromachining uses manufacturing processes originally developed for the microelectronics industry to build mechanical structures with micron- to nanometer-scale features with excellent repeatability and low unit cost. The uniform, slit-shaped structures of the native kidney glomerulus optimize the permeability and selectivity of the filtration process.[4] A novel slit-pore UF membrane based on the seminal microfabrication techniques of Dr. Mauro Ferrari reproduced the idea of the glomerulus in an array of uniform, slit-shaped pores.[5] The permeability and selectivity of the silicon nanopore membranes eliminate the need for mechanical pumps and rely instead on cardiac perfusion pressure to drive UF.

Long-term function of an implanted device is largely dictated by blood–material interactions. Thrombosis is the dominant concern in blood-contacting devices, such as mechanical circulatory support, cardiac valves, and vascular conduits. One simplifying paradigm models thrombosis as being initiated by plasma protein adsorption to artificial surfaces followed by conformational change in adsorbed proteins, platelet binding, and activation of the coagulation cascade. Chemical surface modification with highly hydrated organic polymers can block the initiating step of protein binding.

In addition to material surface chemistry, blood flow in medical devices can determine patterns of thrombosis and failure. Low shear regions of blood flow can lead to stasis-induced thrombosis. Conversely, high shear environments can activate platelets and prime

them to accelerate thrombosis at distant sites.[6] Consequently, the blood biocompatibility of cartridges housing silicon nanopore membranes was considered at two distinct length scales: first, the nanometer scale over which chemical interactions between blood and artificial materials occur, and second, the millimeter scale where fluid dynamics dictate shear stresses on blood components. The goals of these initial experiments in animals were twofold: first, to test whether *in silico* predictions and *in vitro* measurements of pulsatile blood flow and wall shear stress in the hemofilter cartridge were adequate to predict thrombus formation, and second, whether simple hydrophilic polymers could retard protein adhesion and thrombus formation at the membrane surface. In this study, polyethylene glycol (PEG) surface chemistry modified the silicon nanopore membranes to produce a low fouling nonthrombogenic surface7 and computational fluid dynamics simulations guided blood conduit design to avoid regions of recirculation or high shear stress.[8] This framework guided the design, manufacture, and optimization of the function of hemofilter membranes and subsequent testing in animals.

Methods

Silicon Nanopore Membranes

Silicon nanopore membranes were fabricated and surfaced-modified with PEG as previously described (Figure 1).[9] A lot of virgin, prime grade, single side polished, 100 mm-diameter, 500 μm-thick, <100>-oriented, n-type, silicon (Si) wafers was cleaned using a conventional "piranha" clean procedure, which involved a 20 minute immersion in 3:1 H_2SO_4/H_2O_2 mixture, followed by thorough rinsing in deionized water and drying with nitrogen gas. The wafers were further cleaned using a dual-stage RCA clean procedure, which removed any residual surface organic and inorganic contaminants. A 500 nm-thick film of polysilicon was then deposited on the wafer by low-pressure chemical vapor deposition and oxidized to form a 250 nm-thick layer of SiO_2. The oxide layer on the front side of the wafer was patterned by photolithography and wet etching. The backside of the wafer was patterned by reactive etching in chlorine plasma. The resulting pattern consists of approximately 400 nm-wide spaces and lines. Thermal oxidation of the patterned polysilicon was performed to grow a thin sacrificial SiO_2 layer whose thickness defines the pore size of the membrane. The thickness of this conformal SiO_2 film can be readily designed down to 5 nm with <1% variation in critical dimension across a 10 cm-diameter wafer. After a subsequent polysilicon deposition followed by dry etching, the surface of the wafer was exposed to reveal the thin veins of sacrificial oxide sandwiched between polysilicon layers. Afterward, the wafer backside was patterned using deep reactive ion etching to create suspended polysilicon films. The sacrificial oxide was then etched away in the final step of the fabrication process to leave behind open slit-shaped pores in the polysilicon layer. Polyethylene glycol (MW460-590 Da) was covalently bound to the polysilicon surface *via* a silane linkage using a solution-phase technique as previously described.[10]

Membrane hydraulic permeability was measured by filtering phosphate-buffered saline through the device at specific transmembrane pressures and measuring mass accumulation on an analytical balance. Critical dimension of the membrane slit pores was estimated from hydraulic permeability assuming Poiseuille flow. Macromolecular permeability was assessed

in vitro using . Ficoll 70 and Ficoll 400 are polydisperse globular polysaccharides ranging from 2 to 40 nm diameter, which have been used as probes of glomerular permeability. Ficolls were labeled with fluorescein isothiocyanate (Sigma, St. Louis, MO) after the method of Ohlson.[11] Feed and filtrate were analyzed by size exclusion chromatography and size-specific sieving coefficients calculated from the filtrate or feed quotient as previously described.[12]

Cartridge Design and Manufacturing

Candidate conduit geometries that transformed the round pipe flow of a blood vessel to the rectangular duct flow of a parallel-plate hemofilter were sketched in CAD software (Solidworks, Dassault Systemes SOLIDWORKS Corp., Waltham, MA). An optimal final blood flow path geometry with antiparallel ports for blood entry and exit (*i.e.*, a hilum) to facilitate anastomosis to adjacent artery and vein was selected based on computational fluid dynamics models of blood flow (Figure 2, left panels). Sham cartridges with a blood conduit but no membranes (Figure 2, right panel) and cartridges with mounting fixtures for silicon membranes (Figure 3, left panel) were prototyped from medical-grade polycarbonate (Lexan HPS6-1125, Sabic Inc, Pittsfield, MA; machining by Hayes Manufacturing, Inc., Sunnyvale, CA).

Animal Surgery

Vanderbilt University's Institutional Animal Care and Use Committee approved the operative protocol for hemofilter cartridge implantation in class A dogs. The animals were anesthetized with isoflurane. A total of 100 international unit (IU)/kg unfractionated heparin was administered as a bolus at the time of vascular isolation to achieve adequate levels of anticoagulation throughout the surgery. An upper midline laparotomy incision was made to gain entry into the peritoneal cavity. A combination of blunt and sharp dissection was performed to medially rotate the abdominal viscera to expose the left retroperitoneum, aorta, and inferior vena cava (IVC). The aorta and IVC were dissected free of surrounding tissue. Before placing a vascular clamp on the aorta to perform the atrial anastomosis, an additional 1,000 IU of heparin was administered. Seven millimeter-ringed polytetrafluoroethylene (PTFE) grafts were used to create the venous and arterial anastomosis to the IVC and aorta, respectively. The graft length was approximately 2.5–3.0 cm for each vascular anastomosis. The arterial inflow and venous outflow PTFE grafts were connected to the hemofilter. Blood flow was established through the hemofilter. The hemofilter was secured to the psoas muscle adjacent to the inferior pole of the left kidney in the retroperitoneum. Two separate effluent reservoir bags that collect filtered fluid from across each membrane were placed in the upper abdomen (Figure 3). Hemostasis was ensured, and the midline incision was reapproximated and sutured.

Postoperatively, the animals were housed without restrictions. Each animal received 1.5 mg/kg of acetylsalicylic acid orally twice each day. Blood velocities in the grafts were measured with Doppler ultrasound to estimate blood flow through the hemofilter. Centerline velocities were recorded over multiple cardiac cycles and integrated to estimate time-averaged blood velocity, and assuming Poiseuille flow, volumetric flow rate. On postoperative day 3 (n = 2), 4 (n = 2), 5 (n = 1), or 8 (n = 1), the animal was placed under

general anesthetic and the hemofilter and effluent reservoir bags were retrieved. At the completion of the explantation, the animal was euthanized with pentobarbital while under anesthesia.

After explantation, all membranes were examined by light microscopy for defects. Albumin, hemoglobin, and lactate dehydrogenase (LDH) were measured before surgery and at explant in animals 4, 5, and 6 by drawing samples from intravenous catheters. Albumin sieving coefficient was calculated from the ratio of albumin concentration in the filtrate divided by the albumin concentration in the blood. Random samples of each lobe of both lungs were excised after sacrifice and placed in formalin, embedded in paraffin, sectioned, and stained with hematoxylin and eosin.

Results

Nano- and microfabrication processes resulted in 1 1 cm silicon chips bearing 430 nm-thick nanopore membranes with total membrane area 3.6 10^{-5} m^2 (36 mm^2) (Figure 1). Estimated pore sizes in PEG-coated silicon nanopore membranes were similar to design targets of 5–7 nm (Table 1). *In vitro* sieving measurements demonstrated size-dependent retention of macromolecules (Table 1). Benchtop filtration rates at 103 mm Hg averaged 1.0 μl/min. All experimental animals tolerated the procedure well. Mean preoperative weight was 25.3 ± 1.86 kg, and mean weight gain over the course of the experiment was −0.2 ± 0.2 kg. One animal limped for a day after the surgery and was thought to have a transient nerve compression related to positioning during surgery. The limp spontaneously resolved. There was no evidence for severe hemolysis or high-output heart failure, such as volume overload, in any animal. In the three animals in which membranes remained intact, there was a trend toward increase in serum LDH from before the implant to time of explant (65.3 ± 4.7 IU *vs.* 175 ± 56 IU, $p > 0.05$ by t-test) and a trend toward decrease in hemoglobin (17.5 ± 0.4 g/L *vs.* 13.9 ± 1.0 g/L, $p > 0.05$). Histologic examination of wedge biopsies of each lobe of each animal's lungs revealed normal lung architectures with occasional atelectasis. One biopsy showed an organizing thrombus that was several days old at the time of explant. This thromboembolus was in the same animal that evinced the transient limp, raising the possibility that the thromboembolus arose from that limb.

All cartridges had continuous blood flow without thrombosis. Peak blood flow velocities in the cartridge as measured by Doppler ultrasound were between 300 cm/sec, corresponding to a time-averaged volumetric flow of approximately 900 ml/min. There was no clear evidence of a time trend in blood flow rate from postoperative day 1 to time of explant.

At explant, animals 1–3 with experimental durations 4–8 days had much larger total volumes of filtered fluid (30–50 ml) than predicted from *in vitro* measurements (3–8 ml). Filtrate albumin concentrations in these experiments were higher than predicted ($\theta \sim 0.5 - 0.8$) and higher than the 4 nm Ficoll sieving coefficients measured *in vitro* (Table 1). In animals 1–3 where UF rates and albumin sieving coefficients were higher than predicted, small areas where the silicon membrane appeared to have delaminated from its supporting structure were identified by light microscopy. We hypothesized that some time-dependent factor, as yet unknown, was leading to device failure after multiple days. Silicon nanopore

membranes were implanted over shorter 2 to 3 day durations in animals 3–6. Albumin sieving coefficients in animals 3–6 ($\theta \sim 0.23 - 0.30$) were similar to predictions from preimplant filtration tests using globular polysaccharides (Table 1).

Discussion

The major barriers to clinical success of permanently implanted hemofiltration are thrombosis and fouling. *In vitro*, some protein fouling does occur immediately and appears self-limited.[4,9] The technique for blood biocompatibility in these experiments, PEG, is a highly hydrated polymer that blocks protein adsorption to surfaces and does not promote thrombosis or complement activation.[7] Polyethylene glycol was chosen for this set of experiments because there is a simple solution-phase procedure available to bond PEG to silicon.[10,13] Unfortunately, PEG undergoes hydrolysis in aqueous solutions, so experiments are limited to days to weeks at most. Other polymer coatings appear to provide stable interfaces between blood and materials at the cost of more complex coating procedures.[7,14]

The observed UF rates and pore sizes calculated from observed hydraulic permeability generally were in good agreement with design goals and sieving coefficients of albumin and globular polysaccharides. Peritoneal patients on dialysis tolerate dialytic albumin losses on the order of 4 g per day or 2.7 mg/min.[15] For an implanted hemofilter device, assuming no tubular uptake of albumin, an albumin sieving coefficient around 0.1% will be necessary. In prior work, albumin sieving coefficients below the level of detection of the instrumentation have been observed from silicon nanopore membranes with smaller pore sizes than those tested here.[16]

The observation that in a series of experiments, membranes suffered localized mechanical failures that had not been previously observed in bench testing is noteworthy. Silicon film membranes are brittle ceramic-like materials that do not appear to undergo progressive fatigue-based failure, but instead are best described by a probabilistic failure analysis.[17,18] The concern that a small failure, presumably attributable to a manufacturing process variation, would result in catastrophic failure and exsanguination is not supported by the results here. The consequence of membrane fracture appears to be limited in the short term by a self-sealing microscopic thrombus. The mechanisms by which the first implanted hemofilters failed remain unclear but are thought to be an undetected flaw in the silicon processing. The pattern of damage, namely, localized punch through between adjacent pores at apparently random locations in the membrane, was unlike damage patterns observed with overpressure or rough handling that are characterized by large fractures, typically at membrane edges. The mechanisms by which the failures were related to implant duration are unknown.

Nevertheless, the use of cardiac perfusion pressure to enable continuous and selective hemofiltration by silicon nanopore membranes without external connections or implanted power supply is a significant achievement. Pump-free operation decreases the overall size of the implantable device and increases the likelihood of success of long-term operation by eliminating the need for bulky (and toxic) batteries or transcutaneous (and infection-prone) connections. Just as significant is the ability of the hemofilter to operate without chronic,

long-term systemic anticoagulation, which is generally required with any implanted blood-contacting device. Longer implantation periods and larger devices are required to definitively establish whether the hemofilter can operate without any anticoagulation whatsoever. A range of 5–7 mm PTFE grafts used in vascular surgery have excellent patency rates, whereas those used in hemodialysis access may be more problematic. Other groups have used similar diameter vascular grafts to engineer vascularized implants, highlighting the long-term feasibility of this strategy.[19,20] The possibility of avoiding systemic anticoagulation minimizes the risks such as hemorrhage and thrombocytopenia associated with renal replacement therapy.

The key findings of this manuscript are that in a small pilot and feasibility study in animals, the hemofiltration cartridge remained patent and thrombus free with only aspirin as an anticoagulant. The silicon membranes that remained intact during the experiments retained albumin, matching preimplantation measurements with Ficoll. The minimum diameter of a blood conduit, between 4 and 5 mm, and the perfusion pressure of the animal, around 100 mm Hg, caused high blood flow rates through the cartridge. The very high blood flow rate and consequently high shear rates at the membrane surface achieved by this cartridge design are not representative of the operating point of a full-scale cartridge, which will have lower total blood flow and lower shear rates at the membrane face. This feasibility study of an implanted hemofiltration membrane for renal replacement therapy based on a novel biomimetic silicon membrane justifies design engineering of cartridge designs scaled to deliver clinically relevant filtration volumes.

Acknowledgments

This research was supported by 1R01EB008049, 1R01EB014315, and the generous philanthropy of the Wildwood Foundation, the John and Marcia Goldman Foundation, and NIH.

Preliminary results regarding the work in this manuscript were presented in abstract form at the American Society of Nephrology Kidney Week meeting in Philadelphia, Pennsylvania, on November 2014.

Funding Sources: NIH, The Wildwood Foundation, The John and Marcia Goldman

References

1. Tumlin J, Wali R, Williams W, et al. Efficacy and safety of renal tubule cell therapy for acute renal failure. J Am Soc Nephrol. 2008; 19:1034–1040. [PubMed: 18272842]
2. Ronco C, Bowry S. Nanoscale modulation of the pore dimensions, size distribution and structure of a new polysulfone-based high-flux dialysis membrane. Int J Artif Organs. 2001; 24:726–735. [PubMed: 11817320]
3. Nissenson AR, Ronco C. Nanotechnology and dialysis. Int J Artif Organs. 2004; 27:3–5. [PubMed: 14984176]
4. Kanani DM, Fissell WH, Roy S, Dubnisheva A, Fleischman A, Zydney AL. Permeability-selectivity analysis for ultrafiltration: Effect of pore geometry. J Memb Sci. 2010; 349:405. [PubMed: 20161691]
5. Desai TA, Hansford DJ, Kulinsky L, et al. Nanopore technology for biomedical applications. Biomed Microdevices. 1999; 2:11–40.
6. Raz S, Einav S, Alemu Y, Bluestein D. DPIV prediction of flow induced platelet activation-comparison to numerical predictions. Ann Biomed Eng. 2007; 35:493–504. [PubMed: 17286206]
7. Muthusubramaniam L, Lowe R, Fissell WH, et al. Hemocompatibility of silicon-based substrates for biomedical implant applications. Ann Biomed Eng. 2011; 39:1296–1305. [PubMed: 21287275]

8. Yamaguchi T, Ishikawa T, Imai Y, et al. Particle-based methods for multiscale modeling of blood flow in the circulation and in devices: Challenges and future directions. Sixth international bio-fluid mechanics symposium and workshop March 28–30, 2008 Pasadena, California Ann Biomed Eng. 2010; 38:1225–1235. [PubMed: 20336827]
9. Fissell WH, Dubnisheva A, Eldridge AN, Fleischman AJ, Zydney AL, Roy S. High-performance silicon nanopore hemofiltration membranes. J Memb Sci. 2009; 326:58–63. [PubMed: 20054402]
10. Papra A, Gadegaard N, Larsen NB. Characterization of ultrathin poly(ethylene glycol) monolayers on silicon substrates. Langmuir. 2001; 17:1457–1460.
11. Ohlson M, Sorensson J, Haraldsson B. Glomerular size and charge selectivity in the rat as revealed by FITC-ficoll and albumin. Am J Physiol Renal Physiol. 2000; 279:F84–F91. [PubMed: 10894790]
12. Fissell WH, Manley S, Dubnisheva A, et al. Ficoll is not a rigid sphere. Am J Physiol Renal Physiol. 2007; 293:F1209–13. [PubMed: 17652374]
13. Melvin ME, Fissell WH, Roy S, Brown DL. Silicon induces minimal thromboinflammatory response during 28-day intravascular implant testing. ASAIO J. 2010; 56:344–348. [PubMed: 20431483]
14. Li L, Marchant RE, Dubnisheva A, Roy S, Fissell WH. Anti-biofouling Sulfobetaine Polymer Thin Films on Silicon and Silicon Nanopore Membranes. J Biomater Sci Polym Ed. 2011; 22:91–106. [PubMed: 20546677]
15. Balafa O, Halbesma N, Struijk DG, Dekker FW, Krediet RT. Peritoneal albumin and protein losses do not predict outcome in peritoneal dialysis patients. Clin J Am Soc Nephrol. 2011; 6:561–566. [PubMed: 21071518]
16. Fissell W, Zydney A, Groszek J, Ferrell N, Roy S. Enhanced 2-microglobulin clearance by silicon nanopore membranes. JASN. 2010; 21:358A.
17. Jadaan OM, Nemeth NN, Bagdahn J, Sharpe W. Probabilistic weibull behavior and mechanical properties of MEMS brittle materials. J Mater Sci. 2003; 38:4087–4113.
18. Sharpe WN, Jadaan O, Beheim G, Quinn G, Nemeth N. Fracture strength of silicon carbide microspecimens. J Microelectromech Sys. 2005; 14:903–913.
19. Maki T, Mullon CJ, Solomon BA, Monaco AP. Novel delivery of pancreatic islet cells to treat insulin-dependent diabetes mellitus. Clin Pharmacokinet. 1995; 28:471–482. [PubMed: 7656505]
20. Tiranathanagul K, Yossundharakul C, Techawathanawanna N, et al. Comparison of middle-molecule clearance between convective control double high-flux hemodiafiltration and on-line hemodiafiltration. Int J Artif Organs. 2007; 30:1090–1097. [PubMed: 18203071]

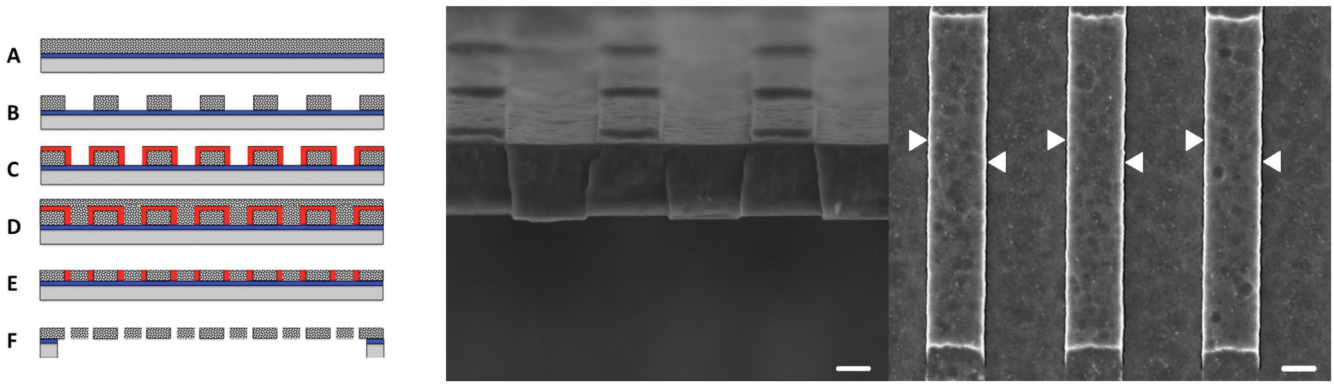

Figure 1.

Left Panel: Cartoon highlighting key steps in the membrane fabrication process. **A**: Thin layers of silicon dioxide (blue) and polycrystalline silicon ("polysilicon", stippled gray) are deposited on a silicon wafer (gray). **B**: The polysilicon layer is patterned into parallel bars using standard photolithography. **C**: A 5–7 nm-thick conformal layer of silicon oxide (red) is grown on the polysilicon. **D**: A second layer of polysilicon is deposited (stippled gray). **E**: The surface is planarized and thinned to expose the 5–7 nm veins of silicon oxide (red). **F**: The oxide is etched away to create 5–7 nm pores, and windows are etched into the wafer to expose the backside of the thin-film membrane. Center Panel: Scanning electron micrograph of cross section of flat sheet silicon nanopore membrane. The 5–7 nm pores (sizes estimated from hydraulic permeability; see text) are the dark marks separating the trapezoid-shaped silicon bars. Scale bar = 200 nm. Right Panel: Scanning electron micrograph of a flat sheet silicon nanopore membrane. Six pores are seen as elongated dark slits to the left and right of three silicon bars (arrowheads). Scale bar = 200 nm.

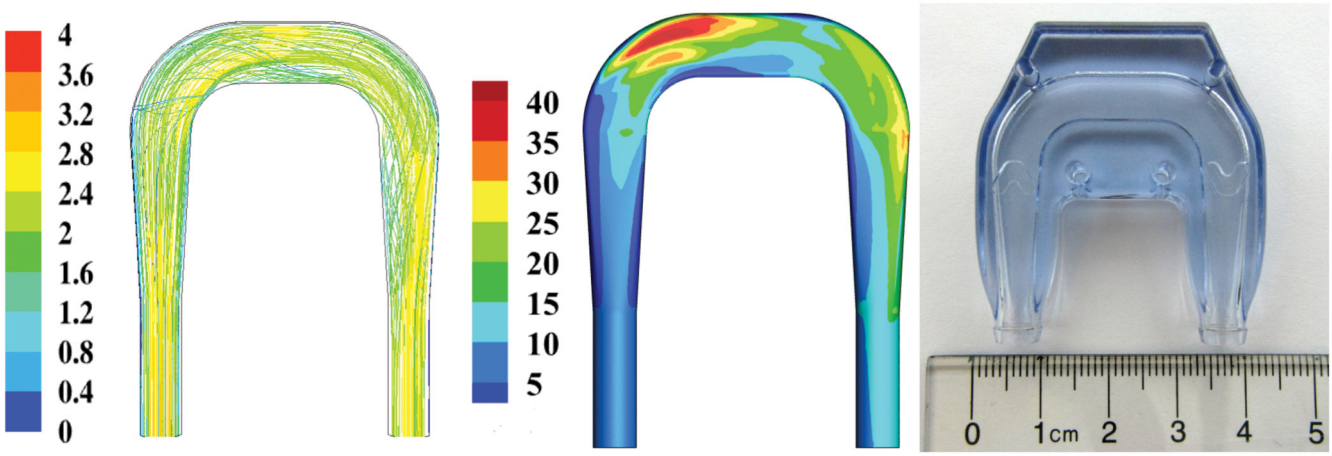

Figure 2.

Left: Computational fluid dynamic (CFD) models of blood flow through hemofilter cartridge. Streamlines are colored by velocity (color scale, units in m/sec) and show uniform flow. Center: CFD predicted wall shear stress (color scale, units in Pa) in hemofilter cartridge. Right: polycarbonate model of blood flow path.

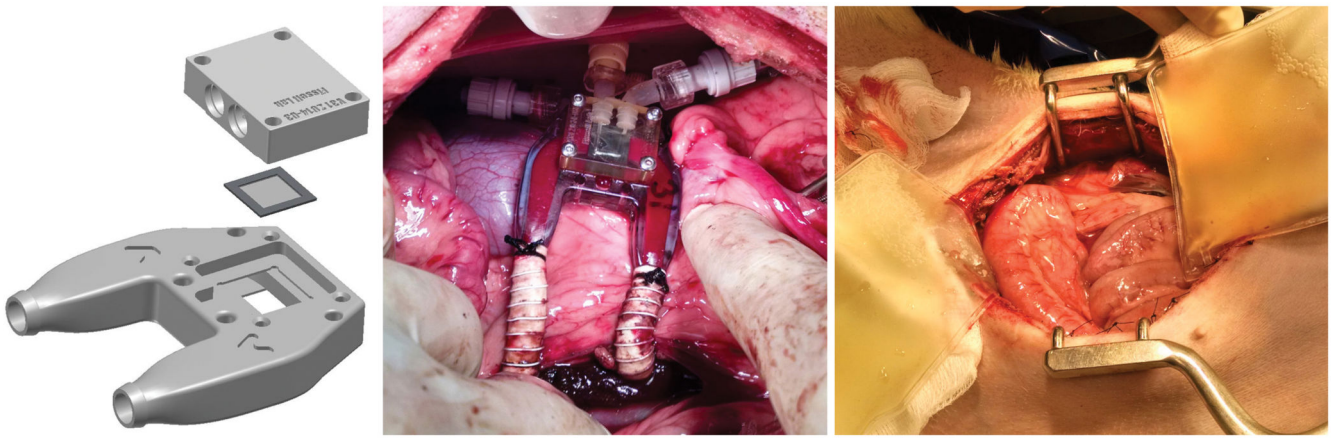

Figure 3.

Left: Exploded view of small scale hemofilter cartridge. The blood flow path is machined into the housing (bottom), which receives the silicon nanopore membrane (middle) and is retained by a cap which drains ultrafiltrate (top). The SNMis sealed to the cartridge by silicone gaskets (not shown). Center: Polycarbonate hemofiltration cartridge at the time of implantation. The cartridge is connected to aorta and vena cava by short 6 mm-diameter polytetrafluoroethylene (PTFE) grafts. Ultrafiltrate from the silicon filters is drained to collection pouches located above the field of view. Right: Ultrafiltrate collection pouches at the time of explant on postoperative day 5. Clear yellow ultrafiltrate without blood is present in both pouches.

ASAIO J. Author manuscript; available in PMC 2017 July 01.

Table 1

Expected and Observed Permselectivity of Implanted Silicon Nanopore Membrane Filters

Animal	Membrane	Pore Size (nm)	Sieving Coefficient			Implant Duration (days)	Filtrate Volume (ml)
			Predicted	40 nm Ficoll Observed	Albumin Observed		
1	A	5.59	0.20		0.516	8	27.5
2	A	6.81	0.38	0.36	0.74	5	50
2	B	6.81	0.38	0.39	0.74	5	40
3	A	7.14	0.42	0.46	0.73	4	22
4	A	5.01	0.09	0.27	0.23	3	5
4	B	5.94	0.26	0.19	0.26	3	8
5	A	6.10	0.28	0.33	0.30	4	4
5	B	6.31	0.51	0.31	0.27	4	5.5
6	A	7.30	0.43		0.3	3	1

For the first three animals, predicted and observed Ficoll sieving were in broad agreement, but membranes leaked albumin *in vivo* to a much greater extent than predicted. Indeed, defects in the membranes were noted at explant. In the final three animals, predicted and observed solute sieving was in closer agreement. For membrane 4A, the pore size estimate is almost certainly inaccurate as the membrane was fabricated on the same wafer as membrane 4B.11